Cell speed, persistence and information transmission during signal relay and collective migration

Colin P. McCann[1,2], Paul W. Kriebel[2], Carole A. Parent[2,*] and Wolfgang Losert[1,2]

[1]Department of Physics, University of Maryland College Park, College Park, MD 20742-4111, USA
[2]Laboratory of Cellular and Molecular Biology, Center for Cancer Research, NCI, NIH, 37 Convent Drive, Bethesda, MD 20892-4255, USA
*Author for correspondence (parentc@mail.nih.gov)

Accepted 1 March 2010
Journal of Cell Science 123, 1724-1731

doi:10.1242/jcs.060137

Summary

Collective migration is a key feature of the social amoebae *Dictyostelium discoideum*, where the binding of chemoattractants leads to the production and secretion of additional chemoattractant and the relay of the signal to neighboring cells. This then guides cells to migrate collectively in a head-to-tail fashion. We used mutants that were defective in signal relay to elucidate which quantitative metrics of cell migration are most strongly affected by signal relay and collective motion. We show that neither signal relay nor collective motion markedly impact the speed of cell migration. Cells maintained a preferred overall direction of motion for several minutes with similar persistence, regardless of whether or not they were attracted to moving neighbors, moving collectively in contact with their neighbors, or simply following a fixed exogenous signal. We quantitatively establish that signal relay not only increases the number of cells that respond to a chemotactic signal, but most remarkably, also transmits information about the location of the source accurately over large distances, independently of the strength of the exogenous signal. We envision that signal relay has a similar key role in the migration of a variety of chemotaxing mammalian cells that can relay chemoattractant signals.

Key words: Chemotaxis, *Dictyostelium discoideum*, Collective migration

Introduction

The ability of cells to migrate directionally in the presence of gradients of chemoattractants, referred to as chemotaxis, is a fundamental physiological response regulating a wide variety of biological processes (Ridley et al., 2003). In fast-moving cells, such as neutrophils and *Dictyostelium discoideum*, chemotaxis is mediated by the binding of chemoattractants to specific G-protein-coupled receptors (GPCRs), which transduce the chemotactic information to several effectors. This eventually leads to the anterior enrichment of F-actin for pseudopod extension and the posterior or side accumulation of myosin II for back retraction (Bagorda et al., 2006; Janetopoulos and Firtel, 2008; Stephens et al., 2008). Interestingly, many types of cells amplify chemotactic signals by synthesizing and secreting additional attractants upon stimulation – a process that is called signal relay (Garcia and Parent, 2008; Weijer, 2009). By relaying signals to neighboring cells, large numbers of cells can communicate and collectively migrate – a process that is emerging as a potentially important mode of transport in morphogenesis and cancer (Friedl and Gilmour, 2009).

Dictyostelium provides an ideal model system to study signal relay and collective cell migration (Franca-Koh et al., 2006; Annesley and Fisher, 2009; Weijer, 2009). When starved, up to 10^5 *Dictyostelium* cells migrate directionally toward each other to form tight aggregates that eventually differentiate into a resistant structure made of a spore head atop a stalk of vacuolated cells, referred to as the fruiting body. The migration process during aggregation is guided by chemoattractants, where individual cells exquisitely sense and migrate toward cAMP signals. The binding of cAMP to its specific GPCR cAR1 (cAMP receptor 1) leads to the activation of a variety of intracellular signaling pathways that regulate chemotaxis, gene expression, and the synthesis and secretion of additional cAMP for signal relay (Kimmel and Parent, 2003). Cyclic AMP emitted by individual cells drives groups of cells to self-aggregate if cells are sufficiently close to each other. Indeed, using mathematical modeling, Cohen and Robertson provided evidence that there is a critical density for aggregation (Cohen and Robertson, 1971), and experimental work performed by several researchers established that a minimal cell-cell distance of 60-80 μm is required to sustain aggregation and formation of fruiting bodies (Hashimoto et al., 1975; Gingle, 1976; Raman et al., 1976). Interestingly, as cells sense and migrate towards cAMP signals, they transition from single cell to group migration by aligning in a head-to-tail fashion to form characteristic lines of cells called ‘streams’ (Weijer, 2004). This transition from single to collective cell migration is dependent on the enzyme that generates cAMP, ACA (the adenylyl cyclase expressed in aggregation), and in particular on its enrichment at the back of chemotaxing cells (Kriebel et al., 2003; Kriebel et al., 2008). Cells lacking ACA, or mutant cells that show a loss of ACA enrichment at their back, do not stream during chemotaxis. We proposed that the cAMP signal is released from the back of cells, and as a result specifically leads cells to follow each other in a head-to-tail fashion. In *Dictyostelium*, streaming therefore provides a direct measure of signal relay during chemotaxis.

Recent studies have revisited the question of how chemotactic signals are translated into migration. Steep chemotactic gradients can effectively trigger actin polymerization and dominant pseudopod formation in the direction of the chemical gradient (Firtel and Chung, 2000; Janetopoulos et al., 2004). However, pseudopods also form when cells are exposed to a uniform concentration of chemoattractants during chemokinesis or under shallow chemotactic gradients (Kriebel et al., 2003; Postma et al., 2003; Postma et al., 2004). Under these conditions, pseudopods emerge near each other in a coordinated fashion allowing cells to

Journal of Cell Science

maintain a chosen direction of motion for several minutes through a process called persistence (Andrew and Insall, 2007; Li et al., 2008; Bosgraaf and Van Haastert, 2009). Chemotactic signals of the strength used for cell-cell communication might simply override this natural ability of cells to maintain direction and generate new pseudopods, or take advantage of it and steer cells by biasing the location of naturally occurring pseudopods, as suggested by King and Insall (King and Insall, 2009).

Although previous studies quantified the ability of single cells to migrate towards well-defined chemoattractant gradients (Fisher et al., 1989; Song et al., 2006; Bosgraaf and Van Haastert, 2009), the role of signal relay on a range of chemotactic measurements has not been assessed. We therefore used cells lacking ACA (*aca*$^{-}$), which are specifically defective in signal relay, and compared their ability to migrate with wild type (WT) cells. By tracing the motion of ensembles of thousands of *Dictyostelium* cells, we were able to study how large populations of cells respond in groups during chemotaxis and to elucidate which aspects of cell migration are affected by signal relay and collective behavior. A second, equally important, goal was to develop a simple metric to assess the presence of signal relay that could be applied when no tell-tale signs of signal relay are present. Indeed, a variety of chemotaxing mammalian cells secrete chemoattractants to amplify signals. Although these cells might not show head-to-tail alignment, signal relay could still have a key role in the recruitment and migration of neighboring cells, and a direct measurement would help decipher the role of signal relay in health and disease states.

Results

Short cell-cell distances and small fluid heights are necessary for cells to relay signals during chemotaxis

To provide baseline data for our studies, we first determined the cell-to-cell distance and fluid height for which *Dictyostelium* cells relay signals and migrate collectively. For these experiments, WT cells were allowed to reach the chemotaxis-competent stage (see Materials and Methods), plated on glass chamber coverslips at cell-cell distances varying between 35 and 150 μm, and covered with 0.5-11 mm of buffer (corresponding to 5-600 μl buffer in an eight-well plate). Thousands of cells were observed by time-lapse microscopy, and their ability to collectively migrate was assessed based on visual inspection for the presence of streams that are one or a few cells wide (Fig. 1A). We found that the ability of cells to migrate spontaneously and form streams requires that cells are close to each other, up to a critical cell-cell distance of less than 100 μm (Fig. 1B); as the cell plating density is lowered, the cell population transitions from forming streams to not forming streams. These findings are very similar to cell-cell distances reported for aggregation and fruiting body formation by other investigators (Hashimoto et al., 1975; Gingle, 1976; Raman et al., 1976). To determine whether the absence of streams at large cell-cell distances is due to the inability of cells to sense their neighbors, or to their inability to release cAMP under diluted conditions, we used a micropipette to establish a stable chemoattractant gradient. This essentially creates an artificial aggregation center to induce the release of cAMP by cells near the micropipette and triggers signal relay. The cell density was varied and the capacity of cells to stream was determined at a constant fluid height. As depicted in Fig. 1C, even when migrating toward an external point source of cAMP, cells stopped forming visible streams at the same cell-cell distance as observed during self-aggregation (the fluid height

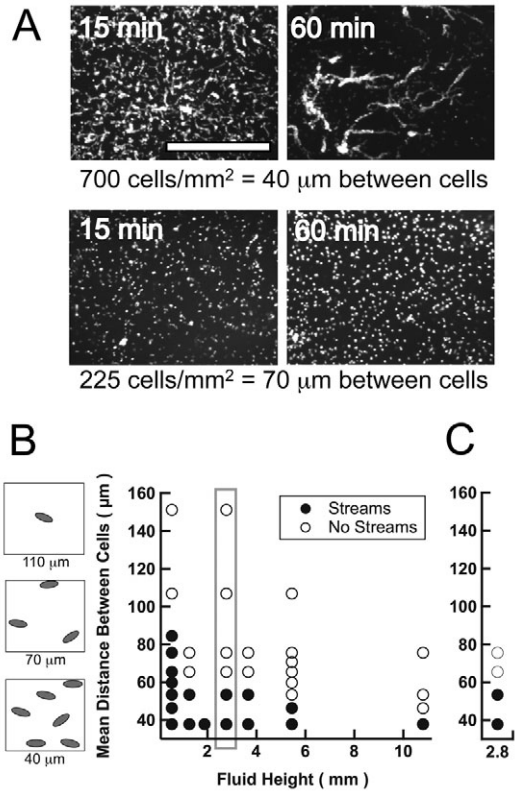

Fig. 1. Short cell-cell distances and small fluid heights are necessary for cells to relay signals during chemotaxis. (**A**) Developed WT *Dictyostelium* cells plated on chambered glass slides at a mean center-to-center distance of ~40 μm (700 cells/mm^2; top images) or a mean distance of ~70 μm between cell centers (225 cells/mm^2; bottom images) under 3.9 mm of buffer. Images were taken with a 5× objective using phase-contrast microscopy 15 and 60 minutes after plating. Scale bar: 500 μm. (**B**) Graph depicting the ability of cells to stream as a function of cell plating densities and fluid heights. Cartoons on left illustrate increasing distance between cells in the vertical direction. Each data point displays the majority result of at least three independent experiments. Grey box indicates region investigated in C. (**C**) Identical experiment as B, but with the addition of a micropipette containing 10 μM cAMP.

highlighted by the box in Fig. 1B is comparable with the fluid height used in Fig. 1C). This finding establishes that the inability of cells to stream is not due to a failure to initiate the production and emission of cAMP. Rather, as previously described by others (Hashimoto et al., 1975; Gingle, 1976; Raman et al., 1976), increasing the distance between cells hinders their capability to sense each other and therefore relay signals.

Fig. 1B shows that the ability of cells to stream also depends on the quantity of fluid present. We observed that when the amount of fluid is increased without changing the cell-cell distance, the cells lose their ability to stream. Remarkably, the addition of medium isolated from high-density WT cells or cells lacking conditioned media factor (CMF) (Gomer et al., 1991) (instead of buffer) recovered streaming (data not shown), suggesting that a secreted factor other than CMF is involved. We envision that the dependence of streaming ability on fluid height, where the extra fluid is present several millimeters away from the cells, is not due to dilution of the cAMP signals for the following reasons: (1) cAMP is not only emitted by cells, but is also degraded via a

secreted phosphodiesterase (Franke and Kessin, 1992), which decreases the distance over which cAMP molecules can travel; (2) cAMP diffuses too slowly [D_{cAMP}=400 μm^2/second (Dworkin and Keller, 1977)] to spread into the extra fluid in significant quantities. This consideration holds true for other signaling molecules larger than cAMP, such as counting factor (CF) (Gao et al., 2002) or CMF. We conclude that molecules smaller than cAMP, such as ions, are more likely to be the source of the fluid volume dependence, because ions diffuse an order of magnitude faster than cAMP (Conkling and Blanchar, 1986). The above argument assumes diffusive transport of molecules or ions; however, strong enough fluid flows could cause dilution of signaling molecules of any size over millimeter distances on the experimental timescales. Thus, fluid flow was minimized during the experiments. Since flows can be triggered by heat and movements involved in imaging multiple wells, we imaged samples only at the start and end of each experiment. Furthermore, we obtained similar findings when cells were plated on agar of varying thickness, where the dense agar gel effectively prevents convective flows (supplementary material Fig. S1) without reducing diffusion (Yuen and Gomer, 1994). However, cAMP dynamics are complex, so we cannot exclude the possibility that cAMP has a role in regulating the dependence of streaming on fluid height. A cell-cell distance of ~40 μm was therefore used for all further experiments as this cell-cell distance allowed signal relay and stream formation under all fluid heights tested.

Signal relay does not regulate individual cell speed and short time persistence

To determine whether the presence of signal relay affects the ability of cells to migrate individually (outside streams), we used *aca*$^-$ cells, which retain the ability to chemotax but do not produce cAMP upon chemoattractant stimulation, and therefore lack the ability to relay signals (Pitt et al., 1992; Kriebel et al., 2003). Both WT and *aca*$^-$ cells were allowed to reach the chemotaxis-competent stage and exposed to a micropipette filled with cAMP as a constant exogenous point source of chemoattractant for chemotaxis measurements. In addition, the behavior of both cell types was studied in the absence of exogenous point sources: *aca*$^-$ cells were exposed to a uniform stimulation of chemoattractant for chemokinesis measurements and WT cells were observed as they spontaneously migrated and aggregated. Indeed, chemokinesis is a key feature of chemotactic migration and is readily observed in *aca*$^-$ cells. WT cells, because of their endogenous ACA activity, do not require further chemoattractant stimulation and spontaneously exhibit random migration (Kriebel et al., 2003). We acquired several time-lapse movies for each condition (see supplementary material Movies 1-4) and automatically extracted the position and motion of all single cells, i.e. before they merged into streams, using custom image-processing routines (see Materials and Methods). To reduce noise and eliminate the contribution of stationary cells, cell speeds were only included from cells that showed a net displacement of 20 μm over a 5 minute time interval. Surprisingly, we found that the speeds of individual cells were comparable for *aca*$^-$ and WT cells (P>0.05) under either chemokinesis, chemotaxis or self-aggregation conditions (Fig. 2A depicts average data of hundreds of cells from one representative movie for each condition; Table 1 shows average speeds of thousands of cells from at least three independent movies once the speed plateau has been reached; see below). We also found that for cells chemotaxing to a point source of chemoattractant, the speed

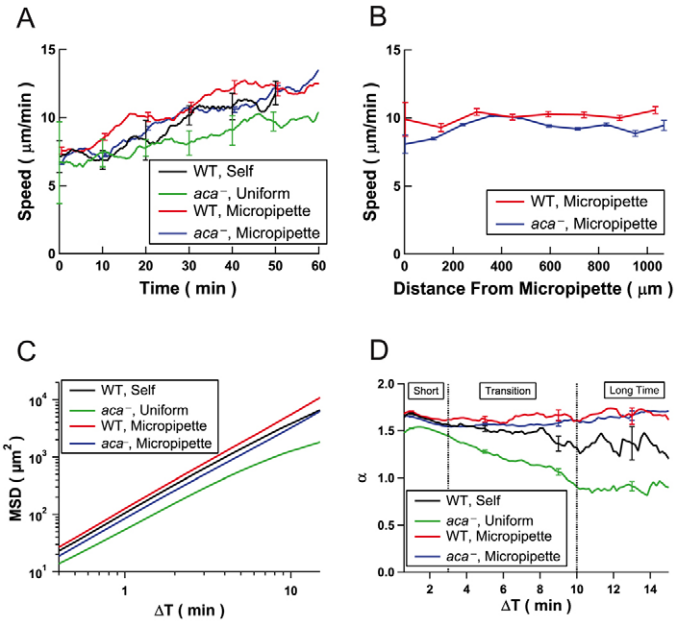

Fig. 2. Signal relay does not regulate cell speed or directional persistence. (**A**) Graph depicting average cell speed versus time for WT and *aca*$^-$ cells. Cells were either subjected to a chemoattractant gradient provided by a micropipette containing 10 μM cAMP (Micropipette) (WT and *aca*$^-$), to a uniform 50 nM cAMP stimulus (Uniform) (*aca*$^-$ cells only), or to endogenous stimulus (Self) (WT cells only). These data are representative of at least three experiments. Error bars indicate s.e.m. (**B**) Graph indicating average speed as a function of distance from a micropipette containing 10 μM cAMP. These data are representative of at least three experiments. Error bars indicate s.e.m. (**C**) Graph depicting MSD measurements as a function of time interval for the experiments presented in A. Error bars indicating s.e. are smaller than the traces and are thus not shown. (**D**) Graph depicting the slope α of the MSD graph in B as a function of time interval for the experiments presented in A. See text for details. Error bars indicate s.e.m. in the average α for every cell. 'Short', 'Transition' and 'Long' designate the ΔT values, where similar, changing and different behaviors are observed between the different experimental conditions (see text).

of moving cells did not depend on the cAMP concentration or gradient, as cell speed did not change as a function of the distance from the micropipette tip (Fig. 2B). Remarkably however, we observed for both WT and *aca*$^-$ cells in all conditions tested that cell speeds almost doubled during the first 60 minutes of migration (Fig. 2A). It is important to note that this gradual increase was distinct from the rapid increase in speed measured just after cells are plated, which was routinely observed. To determine whether the slow increase in cell speed with time was due to development, we starved *aca*$^-$ cells for 5 and 6.5 hours, exposed them to a micropipette, and measured their velocity as a function of time thereafter. We found that neither the absolute speed nor the increase in speed depended on these developmental times, because all conditions displayed similar speeds and behavior (supplementary material Fig. S2). Similarly, cells plated in medium isolated from starving cells showed the same increase in speed (data not shown), suggesting that the accumulation of a secreted factor is not responsible for the gradual increase. Together, these findings establish that signal relay does not regulate individual cells speed during chemotaxis or chemokinesis and that the speed of cells doubles during the first hour of migration.

Table 1. Quantitative migration data of WT and *aca*⁻ cells

Cell type	n[a]	Speed (μm/minute)[b]	α[c]
WT, self-streaming	30±14	10.8±2.2	1.0±0.5
WT, micropipette[d]	78±87	11.7±1.4	1.5±0.1
aca⁻, chemokinesis[e]	50±23	10.7±1.0	1.1±0.2
aca⁻, micropipette[d]	42±44	9.4±0.8	1.5±0.1
Fluorescent WT, self-streaming, outside streams	8±3	11.1±2.9	1.5±0.1
Fluorescent WT, self-streaming, inside streams	31±1	8.9±1.8	1.6±0.1
Fluorescent WT, micropipette[d], outside streams	13±6	10.0±2.5	1.4±0.1
Fluorescent WT, micropipette[d], inside streams	22±19	9.6±1.1	1.5±0.1

[a]Average number ± s.d. of individual cells tracked at each time point for each experiment. Taken from at least three independent experiments.
[b]Speeds (mean ± s.d.) are not statistically different for all conditions tested (P>0.05).
[c]Note that all α (mean ± s.d.) are ~1.6 on short (<1 minute) time intervals.
[d]The micropipette contained 10 μM cAMP.
[e]With the addition of a uniform concentration 50 nM cAMP.

We next measured metrics that indicate how persistent a cell maintains its direction of migration, i.e. the straightness (persistence) of the cell track. This can be readily determined using mean-squared displacement (MSD) measurements, which indicate how far a cell migrates in a given time interval. How fast the MSD increases with time can be seen from the slope of the MSD in the double logarithmic plot of Fig. 2C. The slope provides a measure of persistence, i.e. how well the direction of migration is maintained. In this logarithmic representation, which emphasizes short times, the motion under different conditions has similar slopes and thus similar properties. To measure persistence on longer timescale, we determined the local slope α from Fig. 2C, and plotted it as a function of time interval, as previously described (Dieterich et al., 2008; Takagi et al., 2008) (Fig. 2D). Since it is a derivative, α has higher uncertainty than the MSD (hence the jagged lines compared with Fig. 2C). It nevertheless provides more intuitive insight: cells that move on a straight track would have a slope α of 2 and cover twice the distance when given twice the time, whereas randomly migrating cells would have a slope of 1 and need four times longer (on average) to cover twice the distance. We found that on up to 3 minute timescales ('Short' on Fig. 2D), chemotaxing WT and *aca*⁻ cells have a similar α value, which is consistent with the similar slope of Fig. 2C that highlights short times. The slope of ~1.5 indicated that the overall direction of motion was persistent, but that the cell tracks were not completely straight (Fig. 2D). During chemokinesis of *aca*⁻ cells, the slope α decreased after 3 minutes, leveling off at α values of ~1 at time intervals above 10 minutes ('Long' in Fig. 2D). This indicates that cells without a directional signal maintain a preferred direction over several minutes, but over longer times change direction randomly. By contrast, cells that migrated toward an aggregation center – during spontaneous aggregation or migration to a micropipette – maintained a slope of α = ~1.6 for all timescales, indicating persistence in their direction of motion. Note that persistence data for WT cells had more variation than the data for *aca*⁻ cells (see Table 1). This is because many WT cells quickly joined streams and thus fewer cells could be tracked for the long time intervals needed for MSD measurements.

Together, our findings establish that signal relay does not significantly regulate individual cell speed during chemotaxis and chemokinesis. We also show that although the presence of signal relay or exogenous directional cues does not impact the persistence of individual cells on short timescales, directional cues, regardless of their nature, allow cells to maintain their preferred direction over long times.

Cell speeds and directional persistence are similar inside and outside streams

We next compared the migration behavior of individual cells (outside streams), to the migration ability of cells that are inside streams. Phase-contrast images do not provide clear boundaries between cells in a stream, and thus did not allow us to elucidate the migration of cells within streams. To identify individual cells within a stream, we therefore analyzed WT cell populations where 10% of the cells were treated with Celltracker, a cytosol dye. We captured both fluorescent images to track the position and motion of every tenth cell, and phase-contrast images to track the location and motion of all cells that were not part of a stream, and to elucidate the location of the streams (Fig. 3A and supplementary material Movie 5). Cell speeds were monitored for cells inside and outside streams in the presence or absence of a micropipette containing 10 μM cAMP, as described above. Fig. 3B and Table 1 show that the speed of cells as a function of time was comparable for all cell populations and under all conditions tested (Fig. 3B depicts average data of hundreds of cells from one representative movie; Table 1 shows average speeds of thousands of cells from at least three independent movies once the speed plateau has been reached). The data were again dominated by a significant increase in cell speed over the first hour of migration. Furthermore, the local slope of the MSD (Fig. 3C,D) showed the same degree of directional persistence both inside and outside streams, and this directional persistence was maintained both in spontaneous aggregation and directed migration of WT cells, as noted above. We conclude that directional persistence and cell velocity are not altered when cells transition from single to group migration, even though cell-cell adhesions are present.

Signal relay increases recruitment range and dramatically affects chemotactic index

In our quest to determine the role of signal relay during chemotaxis, we next assessed the recruitment range of WT or *aca*⁻ cells to a point source of chemoattractant. We reasoned that the propagation of chemotactic signals from cell to cell would greatly extend the distance over which a chemotactic signal can travel. We also sought to determine to what degree signal relay between cells can transmit the original information, i.e. whether cells that directly sense an exogenous signal move toward it better than cells 1 mm away that receive a signal relayed by other cells. To answer these questions, chemotactic-competent WT or *aca*⁻ cells were exposed to a micropipette containing various concentrations of cAMP, and their response range (in μm) from the tip of the micropipette was

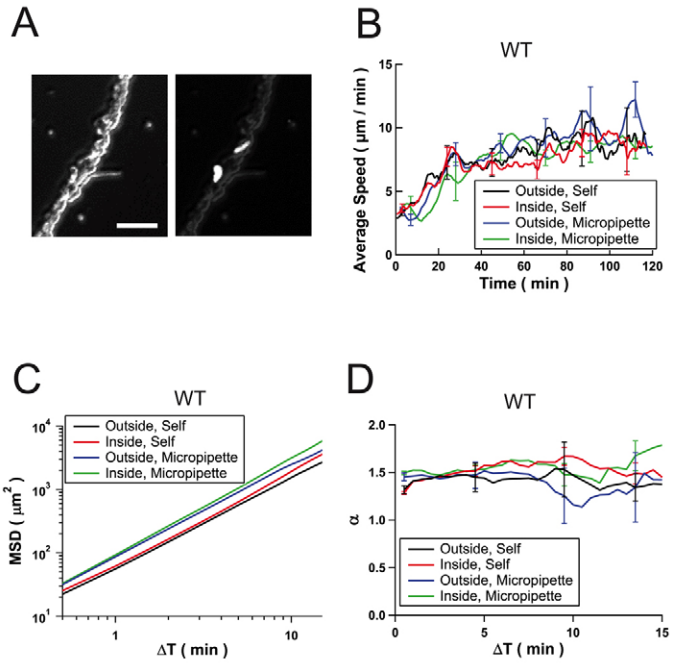

Fig. 3. Cell speeds and directional persistence are similar inside and outside streams. (**A**) (Left) Phase-contrast image of a stream that is several cells wide. (Right) Fluorescent image of the same field overlaid on a darkened phase-contrast image. Two fluorescently dyed cells can be distinguished, and their behavior can be analyzed. Scale bar: 40 μm. (**B**) Graph depicting average cell speed versus time for WT cells inside or outside streams. Cells were either subjected to a chemoattractant gradient provided by a micropipette containing 10 μM cAMP or to an endogenous chemoattractant stimulus. These data are representative of at least three experiments. Error bars indicate s.e.m. (**C**) Graph depicting MSD measurements as a function of time interval for the experiments presented in B. Error bars indicating s.e. are smaller than the traces and are thus not shown. (**D**) Graph depicting the slope α of the MSD graph in C as a function of time interval for the experiments presented in B. See text for details. Error bars indicate s.e.m. of the mean α value for every cell.

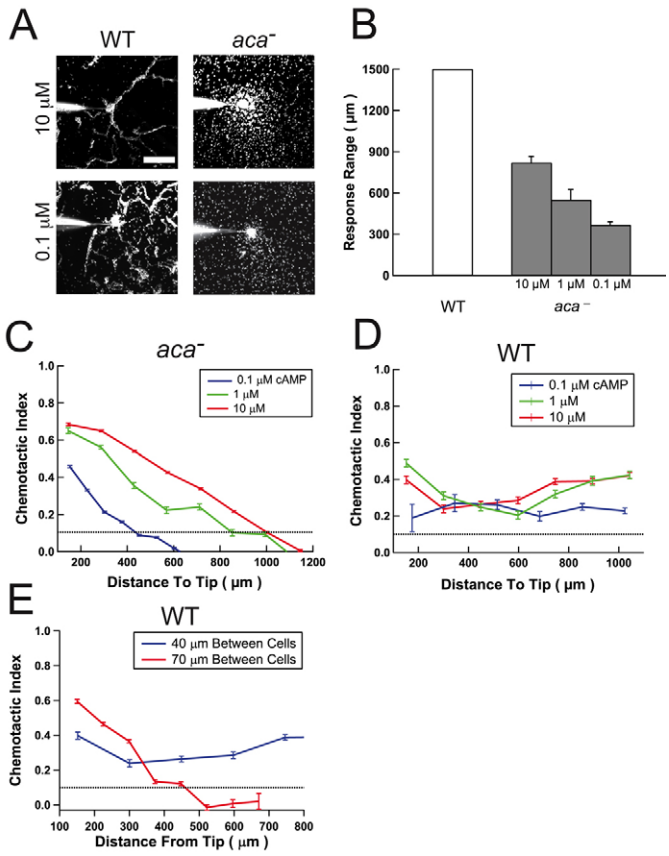

Fig. 4. Signal relay increases recruitment range and regulates the chemotactic index. (**A**) Phase-contrast images of WT or *aca*⁻ cells 60 minutes after the cells started to migrate to a micropipette containing 10 μM (top) or 0.1 μM (bottom) cAMP. Scale bar: 200 μm. (**B**) Quantification of the response range of WT and *aca*⁻ cells over 90 minutes. The numbers on the *x*-axis represent the concentration of cAMP in the micropipette. The method used for determining the response range is presented in C and D. WT cells responded equally to all concentrations tested. Error bars indicate s.e.m. and are derived from three independent experiments. (**C**) Graph depicting the time-averaged CI as a function of the distance from the tip of the micropipette for *aca*⁻ cells migrating to a micropipette containing various concentrations of cAMP. Error bars indicate s.e.m. (**D**) Graph depicting the time-averaged CI as a function of the distance from the tip of the micropipette for WT cells migrating to a micropipette containing various concentrations of cAMP. Error bars indicate s.e.m. (**E**) Graph depicting the time-averaged CI as a function of the distance from the tip of the micropipette for WT cells plated at various densities and migrating to a micropipette containing 10 μM cAMP. In C-E, the dotted line indicates the threshold CI (0.1) used to assess response range in B. Each line indicates a single representative experiment of at least three experiments. Error bars indicate s.e.m.

measured. Fig. 4A shows representative images of WT and *aca*⁻ cells 60 minutes after the activation of the micropipette containing 0.1 μM or 10 μM cAMP and Fig. 4B shows the quantification of the response range to various cAMP concentrations. As expected, *aca*⁻ cells showed a clear dependence of response range on the strength of the cAMP source. With every tenfold increase in cAMP concentration, we measured a ~200 μm (~10 cell length) increase in the response range. However, the response range of WT cells involved the entire visible cell population up to a distance of 1500 μm from the micropipette tip, independently of the cAMP concentration in the micropipette.

The chemotaxis index (CI) of cells provides a measure of how well cell motion is directed toward an exogenous source, and thus a measure of how well the cells sense the 'information' provided by the micropipette. A CI of 1 indicates that a cell is moving directly toward the source and thus fully responds to the information, whereas a CI of 0 indicates motion perpendicular to the direction of the source and thus lack of information about the micropipette position. This analysis was performed on populations of WT or *aca*⁻ cells responding to a micropipette containing 0.1, 1, or 10 μM cAMP. As depicted in Fig. 4C, cells lacking ACA showed a high CI close to the source and a decrease in CI with increasing distance from the micropipette, indicating that sensing of the information provided by the micropipette decreases with distance from the source. Similarly, we found that the CI decreased with decreasing exogenous signal strength for these signal relay-deficient cells. Conversely, as indicated in Fig. 4D, WT cells displayed a constant low CI that was independent of the distance to the micropipette or the amount of chemoattractant signal emitted from the micropipette.

To verify that the CI provided a reliable metric of signal relay rather than just emphasizing the difference between WT and *aca*⁻

cells, we went back to our initial results showing that a minimum cell-cell distance is required for cells to effectively relay signals during migration. In Fig. 1B we showed that increasing the cell-cell distance to 70 μm prevented streaming, even in the presence of an exogenous point source of cAMP, from a micropipette. We now measured the CI for WT cells plated at two cell-cell distances, 40 μm and 70 μm, and subjected to a micropipette containing 10 μM cAMP (Fig. 4E). We found that in the presence of streaming (40 μm cell-cell plating distance) the CI was independent of the distance to the micropipette. By contrast, in the absence of streaming (70 μm cell-cell distance) the CI declined with increasing distance from the micropipette tip. Furthermore, non-streaming cells also showed a higher CI near the micropipette, similar to that measured for *aca*$^{-}$ cells. Together, our findings show that the CI provides meaningful insight into signal relay. In our system, signal relay preserves the information on the location of the micropipette, even at distances where none of the exogenous signal is left, and signals are solely relayed from cell to cell along tens of cells.

Discussion

The ability of cells to propagate chemotactic signals is essential in a wide variety of biological processes and is often associated with the transition from single to collective cell migration. Our study provides novel insight into the behavior of cells exposed to secreted signals during chemotaxis and collective cell migration. We first confirmed that short cell-cell distances are necessary for cells to aggregate and showed that a maximum cell-cell distance of 50-100 μm is necessary for cells to form streams. We reason that for such close neighbors, the specific location on a cell from where the chemotactic signal is emitted during signal relay should matter. Indeed, in *Dictyostelium*, the cellular distribution of signal-relay components is spatially restricted: ACA is enriched at the back of chemotaxing cells, presumably giving rise to localized cAMP secretion and head-to-tail cell alignment (Kriebel et al., 2003). The fact that signal relay occurs over very short distances indicate that such local secretion could impact signal relay. For 20-μm-long polarized cells at center-to-center distances of 100 μm, if signal relay were not from tail to head, an emitted signal would need to cover a 25% longer distance and take roughly 50% longer to cover that distance. Furthermore, additional factors are required to generate directional information via signal relay – if all cells continuously emit cAMP, even a localized release would not generate population-wide directional information in groups of randomly oriented cells. Indeed, in-depth studies of self-aggregation have shown that waves of cAMP are crucial and require three factors: the release of cAMP in bursts, the degradation of cAMP by external phosphodiesterases, and the brief adaptation of the signal-transduction cascade following cAMP sensing and relay (Palsson et al., 1997; Dormann et al., 2002). Although no clear cAMP waves are visible during chemotaxis to a micropipette, the similarity in migration metrics between self-aggregating and chemotaxis to a micropipette suggests that these factors also contribute to the relay of information to an exogenous signal.

We measured the effect of signal relay on a variety of cell-migration parameters and found that neither the speeds of individual moving cells nor their directional persistence is affected by signal relay. We also discovered that individual cell speed significantly increases during the first hour after the start of migration in all conditions tested, and then levels out in the second hour to about twice its initial value. This is consistent with other qualitative observations (Gruver et al., 2008) as well as quantitative analyses of cell speeds during self-aggregation (Rietdorf et al., 1996). We found that the gradual increase in speed was not due to continued development during the course of the experiments and it also appeared to be unrelated to where pseudopods form, because directional persistence did not change significantly with time. Increase in speed also appeared to be unrelated to more effective sensing, because the CI did not change over time. Although the mechanism underlying this remains to be determined, it probably involves an increase in the size or growth rate of pseudopods.

Interestingly, under our experimental settings, cell speed did not depend on the distance from the micropipette. Studies using microfluidic devices have shown that *Dictyostelium* sharply transition from a low basal speed in weak gradients, to a higher speed in strong gradients (Song et al., 2006). This apparent discrepancy can be explained by the fact that the microfluidic and micropipette devices generate different cAMP concentration gradients. Indeed, based on experiments where the micropipette was filled with rhodamine (data not shown), we determined that the cAMP concentration gradients used in our studies were in the high range of cAMP gradients used by Song and colleagues (Song et al., 2006), where the cells moved at constant maximum speed. Our observation that the CI is constant for WT cells indicates that signal relay dominates over the exogenous signal from the micropipette, suggesting that our exogenous gradients are comparable with the concentration gradients generated by cells at the cell-cell distances needed for signal relay and spontaneous aggregation.

We determined how well a cell maintains its direction of migration by measuring how fast the MSD changed as a function of a time interval ΔT. The slope of this graph, α, provides important insights, because it highlights which motility behavior dominates at each timescale. We found that both individual WT and *aca*$^{-}$ cells maintain a preferred direction of motion over ~3 minute intervals under both chemokinesis and chemotaxis conditions, which is consistent with other reports on individual cell migration (Tranquillo et al., 1988; Fisher et al., 1989; Fisher, 1990; Soll et al., 2002; Arrieumerlou and Meyer, 2005; Li et al., 2008; Takagi et al., 2008). This indicates that the tendency of pseudopods to develop close to each other, as suggested by Bosgraaf and van Haastert (Bosgraaf and Van Haastert, 2009), might dominate the dynamics over short times, even during chemotaxis and signal relay. The timescale where α decreases during chemokinesis (3-10 minutes in Fig. 2D) can be interpreted as the time over which the preferred location of pseudopods changes and cells turn. When directional chemotactic cues are present, either from exogenous sources or owing to signal relay, cells maintain a preferred direction over long times, and the slope α thus remains near 1.6. This indicates that chemotactic signals bias the location of naturally occurring pseudopods, as suggested by King and Insall, thus allowing cells to maintain a preferred direction over longer times (King and Insall, 2009).

Remarkably, we found that both cell speed and persistence in the direction of motion are identical in individual cells, as well as in cells inside streams that are one or a few cells wide. This finding was surprising – we expected cells moving in groups to have distinct behaviors, as observed in simulations that explore the role of cell adhesion during early and late stages of morphogenesis (Palsson and Othmer, 2000; Palsson, 2008). Indeed, cell-cell adhesion sites might induce both biochemical and mechanical perturbations (Bowers-Morrow et al., 2004; Weijer, 2009). Our findings therefore establish that the intrinsic motility machinery, as

well as the ability to migrate directionally, are innate properties of single cells that are maintained independently of additional external signals or cell-cell interactions.

Our findings show that signal relay dramatically affects the recruitment range of cells to an exogenous source of chemoattractant. In the absence of signal relay, the range from which cells migrate to the chemotactic source exhibits a strong dependence on the strength of the chemotactic signal. By contrast, in the presence of signal relay, the response range is independent of the cAMP signal strength. CI measurements as a function of distance from the chemoattractant source provide interesting insight into this. As expected, when signal relay is absent (in *aca*$^-$ cells or in diluted WT cells), we find that the CI decreases with distance from an exogenous source, and increases with increasing source strength. When signal relay is present, the CI becomes independent of distance from the exogenous source as well as of its strength. Yet, under these conditions, the CI is significantly smaller than without signal relay close to the chemotactic source. Thus our findings show that signal relay can transmit directional information over long distances without significant information loss. Interestingly, van Haastert and Postma recently reported that WT cells show a decrease in CI with increasing distance from the chemotactic source or with decreasing source strength (van Haastert and Postma, 2007). Based on our extensive analyses, we envision that their experiments were probably performed under dilute conditions where the chemotactic signal is not relayed.

Taken together, our data show that signal relay enhances recruitment range without affecting cell speed or directionality. Although streaming represents a clear indicator of signal relay in *Dictyostelium*, signal relay does not need to give rise to streams. We propose that the independence of the CI on the distance from an exogenous chemoattractant source represents a robust metric to determine whether signal relay takes place in various chemotactic systems. Signal relay during chemotaxis needs to encode directional information, which is achieved through restricted cellular distribution, signal degradation, and refractory periods. We propose that some, if not all, of these features are needed to generate an effective relay of information between neighboring cells. We suggest that the combination of speed, persistence and CI measurements together represent a powerful way to dissect signal relay in motile cells.

Materials and Methods

Cell growth, differentiation and labeling

WT *Dictyostelium discoideum* (strain AX3) and adenylyl cyclase A null (*aca*$^-$) mutant cells (in an AX3 background) were grown in HL-5 medium in exponential phase to 4-5×10^6 cells/ml (Sussman, 1987). For experiments, cells were developed for 4.5 (WT) or 5 hours (*aca*$^-$) in development buffer (DB; 5 mM Na_2HPO_4, 5 mM NaH_2PO_4, pH 6.2, 2 mM $MgSO_4$ and 0.2 mM $CaCl_2$) at 2×10^7 cells/ml, with exogenous pulses of 75 nM cAMP every 6 minutes, as previously described (Devreotes et al., 1987). In some experiments, a fraction of cells was fluorescently labeled by adding 25 μM CellTracker Green CDMFA (Invitrogen) to cells and shaking for 30 minutes, as previously described (Dormann and Weijer, 2006). The cells were then washed twice in DB and mixed at a 1:10 ratio with unlabeled cells.

Microscopy

Cell imaging was performed on a Zeiss Axiovert S100 microscope equipped with a CoolSnap HQ CCD camera (Roper Scientific), using a 2.5× (NA 0.075), 5× (NA 0.16) or 10× (NA 0.3) objective. For 4× images a 1.6× optivar was used with the 2.5× objective. IPLab software (Scanalytics, Fairfax, VA) was used to operate the microscope and camera. Fluorescent light was provided by a FluoArt mercury lamp with appropriate optical filters. Phase-contrast microscopy was used in all non-fluorescent imaging. Phase-contrast imaging was adjusted so that objects (cells and streams) appeared bright on a black background, which provided sufficient contrast for automated tracking routines to easily identify objects.

Chemotaxis assays

In all experiments, cells were taken from development and centrifuged at 9000 r.p.m. for 4 minutes using an Eppendorf microfuge. The supernatant was aspirated and the pellet was washed twice with phosphate buffer (PB; 5 mM Na_2HPO_4, 5 mM NaH_2PO_4, pH 6.2). For density and fluid height self-aggregation studies, cells at the stated concentration were plated onto eight-chamber slides (Lab-Tek, Nunc; dimensions: 7.5 mm width, 7.5 mm length, 11 mm height) and allowed to adhere for 5 minutes. A precise volume of PB was added to achieve the final fluid height. Images were acquired using phase-contrast microscopy. The presence or absence of streams was scored by identifying head-to-tail chains of several cells (~10) in length. For micropipette migration assays, cells at a density of ~40 μm between cells (700 cells/mm^2) were plated onto two-chamber slides (Lab-Tek), allowed to settle for 5 minutes, and 1.5 ml PB was added to reach the final volume. An Eppendorf Femtojet system was used to continuously release cAMP from a Femtojet I micropipette at a pressure of 80 hPa as previously described (Kriebel et al., 2003). At the onset of experiments, a short pulse of high pressure was applied to ensure proper working of the pipette during the course of the experiment. Phase-contrast images were taken every 10 seconds for at least 90 minutes. Fluorescent images were taken using a GFP filter set every 30 seconds immediately following a phase-contrast image. Celltracker concentration and light exposure were minimized and the speeds of fluorescent and non-fluorescent cells in the same experiment were identical (data not shown).

Image analysis

Images were binarized using ImageJ software (NIH). For phase-contrast images, the background was subtracted using a rolling-ball algorithm and the remaining image thresholded. For fluorescent images, bandpassing and thresholding were performed. To identify the position of cells in each frame and track the motion of fluorescent cells from frame to frame, a publicly available algorithm was used (http://physics.georgetown.edu/matlab/). Identification of cells in phase-contrast images, as well as tracking, was carried out using custom Matlab (The Mathworks, Natick, MA) code. This allowed fully automated cell tracking, because the software kept track of individual cells and only counted those cells in the statistics that were not part of a larger group. No subjective measures were used to include or exclude specific cells from the population analyses.

Cell centroids were calculated by finding the center-of-mass of individual objects in the binarized images. These positions were then smoothed using a three-frame (30 second) unweighted sliding window – a time that corresponds to a distance of about 1.5 pixels (at 4× magnification), which is comparable to the uncertainty of our tracking algorithm at this lowest resolution (see below). For fluorescent images, no smoothing was performed, as the time between frames was already 30 seconds.

Velocities were determined by finding the displacement between smoothed center positions in each frame: $\vec{u}_i(t,i) = \vec{x}_i(t) - \vec{x}_i(t-\Delta t)$, where $\vec{x}_i(t)$ is the smoothed centroid of cell i at time t, and Δt is the time between frames. Velocity was only counted in averages during a timeframe where cells had a net displacement of 20 μm over a 5 minute period. This was done to reduce noise and eliminate the contribution of cells that essentially moved in place. After a non-fluorescent cell touched another cell or entered a stream it was ignored, and speeds of streams or other cell groups were not computed. Errors in finding cell centers are presumed to be ≤1 pixel in x and y, and therefore overall $\delta\vec{x}\leq 1.4$ pixels. This corresponds to less than 4.4 μm (at 4× magnification), 3.5 μm (5×) or 1.8 μm (10×). Using smoothed centers presumably reduced this uncertainty further.

The mean square displacement (MSD) gives a measure for the type of motion displayed by cells. This is computed by $\mathrm{MSD}(\Delta T) = \langle \vec{x}_i(t) - \vec{x}_i(t-\tau)\rangle_{t,i}$, where the brackets indicate averages over all times t and all cells i. Unlike the calculation of velocities, cells were only counted if they had a net displacement of 20 μm over the entire cell track. Otherwise, the (stricter) criteria used in calculating velocity introduced an artificial persistence over short timescales. We also note that MSDs that were smaller than the noise value, considered to be one pixel, were ignored. The MSD values were fit to the function $\mathrm{MSD}(\Delta T)=C^*\Delta T^{\alpha}$. The exponent α gives the information about the type of motion that the cell displays: $\alpha=1$ defines diffusive motion, $1<\alpha<2$ is superdiffusive motion and $\alpha=2$ is straight-line motion.

The instantaneous chemotactic index (CI) for cell i at time t is defined as $\mathrm{CI}(t,i) = [\vec{u}_i(t)\circ\hat{r}_i(t)]/|\vec{u}_i(t)| = \cos[\theta_i(t)]$, where $\hat{r}_i(t)$ is the unit direction vector from cell i to the pipette at time t and $\theta_i(t)$ is the angle between the motion vector of cell i at time t and the vector pointing to the pipette. With this definition, CI=1 means a cell is moving directly towards the pipette, CI=0 means a cell is moving perpendicular to the direction to the pipette and CI=–1 means a cell is moving directly away from the pipette.

Signal recruitment range for non-streaming cells was computed by first binning the instantaneous CI of cells in all frames based on distance from the pipette. These indices were then averaged for each bin. When the average CI for a bin was above a certain threshold (0.1), that bin was considered to be directed toward the pipette. The distance from the pipette to the farthest bin above the threshold was considered to be the 'signal range' of the pipette.

The authors would like to thank Alan Kimmel for the use of his microscope for self-aggregation experiments as well as the *Dictyostelium* Stock Center for providing cells lacking CMF. We also

like to thank the Parent and Losert lab members for excellent discussions and in particular Meghan Driscoll for insightful suggestions. W.L. and C.M. acknowledge support from the NIST Center for computational Materials Science and from NSF grant PHY0750371. This research was supported by the Intramural Research Program of the National Institutes of Health, National Cancer Institute, Center for Cancer Research. Deposited in PMC for release after 12 months.

Supplementary material available online at
http://jcs.biologists.org/cgi/content/full/123/10/1724/DC1

References

Andrew, N. and Insall, R. H. (2007). Chemotaxis in shallow gradients is mediated independently of PtdIns 3-kinase by biased choices between random protrusions. *Nat. Cell Biol.* **9**, 193-200.

Annesley, S. J. and Fisher, P. R. (2009). Dictyostelium discoideum-a model for many reasons. *Mol. Cell Biochem.* **329**, 73-91.

Arrieumerlou, C. and Meyer, T. (2005). A local coupling model and compass parameter for eukaryotic chemotaxis. *Dev. Cell* **8**, 215-227.

Bagorda, A., Mihaylov, V. A. and Parent, C. A. (2006). Chemotaxis: moving forward and holding on to the past. *Thromb. Haemost.* **95**, 12-21.

Bosgraaf, L. and Van Haastert, P. J. (2009). Navigation of chemotactic cells by parallel signaling to pseudopod persistence and orientation. *PLoS One* **4**, e6842.

Bowers-Morrow, V. M., Ali, S. O. and Williams, K. L. (2004). Comparison of molecular mechanisms mediating cell contact phenomena in model developmental systems: an exploration of universality. *Biol. Rev. Camb. Philos. Soc.* **79**, 611-642.

Cohen, M. H. and Robertson, A. (1971). Wave propagation in the early stages of aggregation of cellular slime molds. *J. Theor. Biol.* **31**, 101-118.

Conkling, B. and Blanchar, R. (1986). Estimation of calcium diffusion coefficients from electrical conductance. *Soil Sci. Soc. Am. J.* **50**, 1455-1459.

Devreotes, P., Fontana, D., Klein, P. J., S. and Theibert, A. (1987). Transmembrane signaling in *Dictyostelium*. *Methods Cell Biol.* **28**, 299-331.

Dieterich, P., Klages, R., Preuss, R. and Schwab, A. (2008). Anomalous dynamics of cell migration. *Proc. Natl. Acad. Sci. USA* **105**, 459-463.

Dormann, D. and Weijer, C. J. (2006). Visualizing signaling and cell movement during the multicellular stages of dictyostelium development. *Methods Mol. Biol.* **346**, 297-309.

Dormann, D., Vasiev, B. and Weijer, C. J. (2002). Becoming multicelluar by aggregation: The morphogenesis of the social amoebae Dictyostelium discoideum. *J. Biol. Phys.* **28**, 765-780.

Dworkin, M. and Keller, K. H. (1977). Solubility and diffusion coefficient of adenosine 3′:5′-monophosphate. *J. Biol. Chem.* **252**, 864-865.

Firtel, R. A. and Chung, C. Y. (2000). The molecular genetics of chemotaxis: sensing and responding to chemoattractant gradients. *BioEssays* **22**, 603-615.

Fisher, P. R. (1990). Pseudopodium activation and inhibition signals in chemotaxis by Dictyostelium discoideum amoebae. *Semin. Cell Biol.* **1**, 87-97.

Fisher, P. R., Merkl, R. and Gerisch, G. (1989). Quantitative analysis of cell motility and chemotaxis in Dictyostelium discoideum by using an image processing system and a novel chemotaxis chamber providing stationary chemical gradients. *J. Cell Biol.* **108**, 973-984.

Franca-Koh, J., Kamimura, Y. and Devreotes, P. (2006). Navigating signaling networks: chemotaxis in Dictyostelium discoideum. *Curr. Opin. Genet. Dev.* **16**, 333-338.

Franke, J. and Kessin, R. H. (1992). The cyclic nucleotide phosphodiesterases of Dictyostelium discoideum: molecular genetics and biochemistry. *Cell Signal.* **4**, 471-478.

Friedl, P. and Gilmour, D. (2009). Collective cell migration in morphogenesis, regeneration and cancer. *Nat. Rev. Mol. Cell Biol.* **10**, 445-457.

Gao, T., Ehrenman, K., Tang, L., Leippe, M., Brock, D. A. and Gomer, R. H. (2002). Cells respond to and bind countin, a component of a multisubunit cell number counting factor. *J. Biol. Chem.* **277**, 32596-32605.

Garcia, G. L. and Parent, C. A. (2008). Signal relay during chemotaxis. *J. Microsc.* **231**, 529-534.

Gingle, A. R. (1976). Critical density for relaying in Dictyostelium discoideum and its relation to phosphodiesterase secretion into the extracellular medium. *J. Cell Sci.* **20**, 1-20.

Gomer, R. H., Yuen, I. S. and Firtel, R. A. (1991). A secreted 80 × 10(3) Mr protein mediates sensing of cell density and the onset of development in Dictyostelium. *Development* **112**, 269-278.

Gruver, J. S., Wikswo, J. P. and Chung, C. Y. (2008). 3′-phosphoinositides regulate the coordination of speed and accuracy during chemotaxis. *Biophys. J.* **95**, 4057-4067.

Hashimoto, Y., Cohen, M. H. and Robertson, A. (1975). Cell density dependence of the aggregation characteristics of the cellular slime mould Dictyostelium discoideum. *J. Cell Sci.* **19**, 215-229.

Janetopoulos, C. and Firtel, R. A. (2008). Directional sensing during chemotaxis. *FEBS Lett.* **582**, 2075-2085.

Janetopoulos, C., Ma, L., Devreotes, P. N. and Iglesias, P. A. (2004). Chemoattractant-induced phosphatidylinositol 3,4,5-trisphosphate accumulation is spatially amplified and adapts, independent of the actin cytoskeleton. *Proc. Natl. Acad. Sci. USA* **101**, 8951-8956.

Kimmel, A. R. and Parent, C. A. (2003). The signal to move: D. discoideum go orienteering. *Science* **300**, 1525-1527.

King, J. S. and Insall, R. H. (2009). Chemotaxis: finding the way forward with Dictyostelium. *Trends Cell. Biol.* **19**, 523-530.

Kriebel, P. W., Barr, V. A. and Parent, C. A. (2003). Adenylyl cyclase localization regulates streaming during chemotaxis. *Cell* **112**, 549-560.

Kriebel, P. W., Barr, V. A., Rericha, E. C., Zhang, G. and Parent, C. A. (2008). Collective cell migration requires vesicular trafficking for chemoattratant delivery at the trailing edge. *J. Cell Biol.* **183**, 949-961.

Li, L., Norrelykke, S. F. and Cox, E. C. (2008). Persistent cell motion in the absence of external signals: a search strategy for eukaryotic cells. *PLoS One* **3**, e2093.

Palsson, E. (2008). A 3-D model used to explore how cell adhesion and stiffness affect cell sorting and movement in multicellular systems. *J. Theor. Biol.* **254**, 1-13.

Palsson, E. and Othmer, H. G. (2000). A model for individual and collective cell movement in Dictyostelium discoideum. *Proc. Natl. Acad. Sci. USA* **97**, 10448-10453.

Palsson, E., Lee, K. J., Goldstein, R. E., Franke, J., Kessin, R. H. and Cox, E. C. (1997). Selection for spiral waves in the social amoebae Dictyostelium. *Proc. Natl. Acad. Sci. USA* **94**, 13719-13723.

Pitt, G. S., Milona, N., Borleis, J. A., Lin, K. C., Reed, R. R. and Devreotes, P. N. (1992). Structurally distinct and stage-specific adenylyl cyclase genes play different roles in *Dictyostelium* development. *Cell* **69**, 305-315.

Postma, M., Roelofs, J., Goedhart, J., Gadella, T. W., Visser, A. J. and Van Haastert, P. J. (2003). Uniform cAMP stimulation of Dictyostelium cells induces localized patches of signal transduction and pseudopodia. *Mol. Biol. Cell* **14**, 5019-5027.

Postma, M., Roelofs, J., Goedhart, J., Loovers, H. M., Visser, A. J. and Van Haastert, P. J. (2004). Sensitization of Dictyostelium chemotaxis by phosphoinositide-3-kinase-mediated self-organizing signalling patches. *J. Cell Sci.* **117**, 2925-2935.

Raman, R. K., Hashimoto, Y., Cohen, M. H. and Robertson, A. (1976). Differentiation for aggregation in the cellular slime moulds: the emergence of autonomously signalling cells in Dictyostelium discoideum. *J. Cell Sci.* **21**, 243-259.

Ridley, A. J., Schwartz, M. A., Burridge, K., Firtel, R. A., Ginsberg, M. H., Borisy, G., Parsons, J. T. and Horwitz, A. R. (2003). Cell migration: integrating signals from front to back. *Science* **302**, 1704-1709.

Rietdorf, J., Siegert, F. and Weijer, C. J. (1996). Analysis of optical density wave propagation and cell movement during mound formation in Dictyostelium discoideum. *Dev. Biol.* **177**, 427-438.

Soll, D. R., Wessels, D., Heid, P. J. and Zhang, H. (2002). A contextual framework for characterizing motility and chemotaxis mutants in Dictyostelium discoideum. *J. Muscle Res. Cell Motil.* **23**, 659-672.

Song, L., Nadkarni, S. M., Bodeker, H. U., Beta, C., Bae, A., Franck, C., Rappel, W. J., Loomis, W. F. and Bodenschatz, E. (2006). Dictyostelium discoideum chemotaxis: threshold for directed motion. *Eur J. Cell Biol.* **85**, 981-989.

Stephens, L., Milne, L. and Hawkins, P. (2008). Moving towards a better understanding of chemotaxis. *Curr. Biol.* **18**, R485-R494.

Sussman, M. (1987). Cultivation and synchronous morphogenesis of *Dictyostelium* under controlled experimental conditions. *Methods Cell Biol.* **28**, 9-29.

Takagi, H., Sato, M. J., Yanagida, T. and Ueda, M. (2008). Functional analysis of spontaneous cell movement under different physiological conditions. *PLoS One* **3**, e2648.

Tranquillo, R. T., Lauffenburger, D. A. and Zigmond, S. H. (1988). A stochastic model for leukocyte random motility and chemotaxis based on receptor binding fluctuations. *J. Cell Biol.* **106**, 303-309.

van Haastert, P. J. and Postma, M. (2007). Biased random walk by stochastic fluctuations of chemoattractant-receptor interactions at the lower limit of detection. *Biophys. J.* **93**, 1787-1796.

Weijer, C. J. (2004). Dictyostelium morphogenesis. *Curr. Opin. Genet. Dev.* **14**, 392-398.

Weijer, C. J. (2009). Collective cell migration in development. *J. Cell Sci.* **122**, 3215-3223.

Yuen, I. S. and Gomer, R. H. (1994). Cell density-sensing in Dictyostelium by means of the accumulation rate, diffusion coefficient and activity threshold of a protein secreted by starved cells. *J. Theor. Biol.* **167**, 273-282.

A

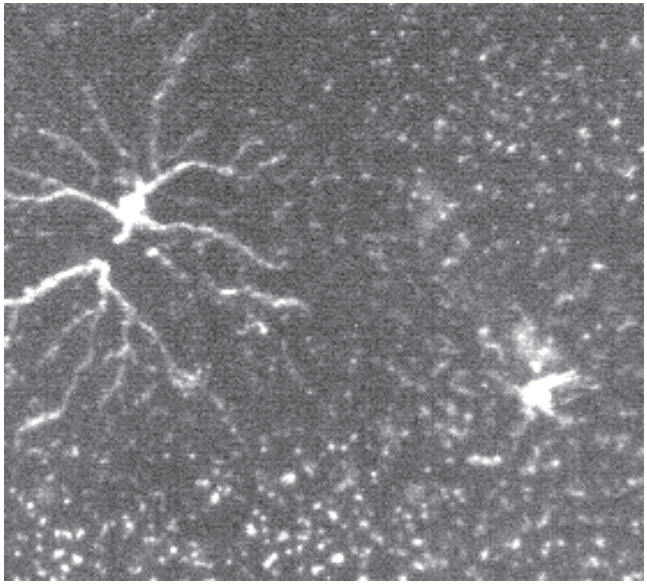

B

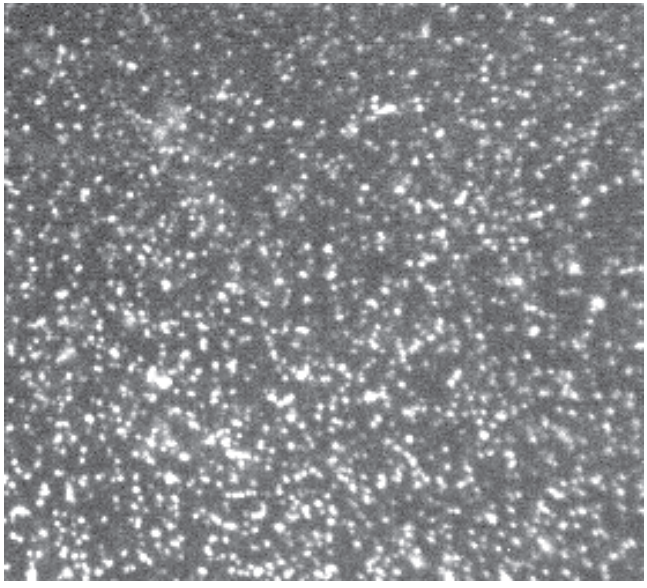

C

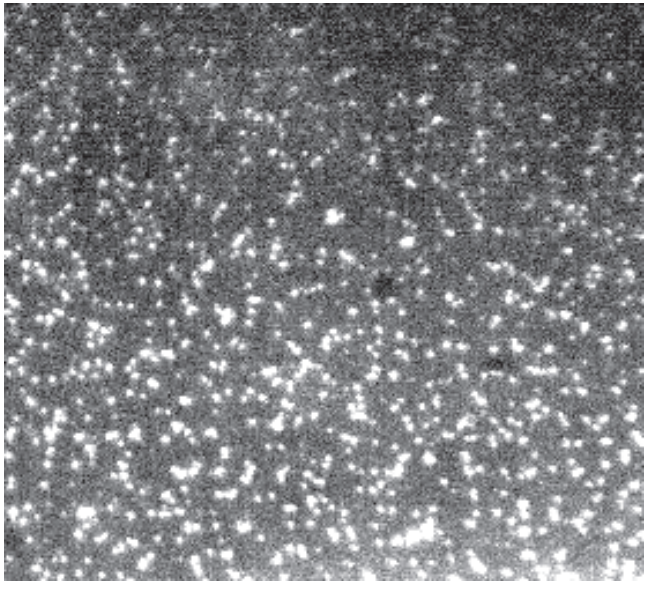

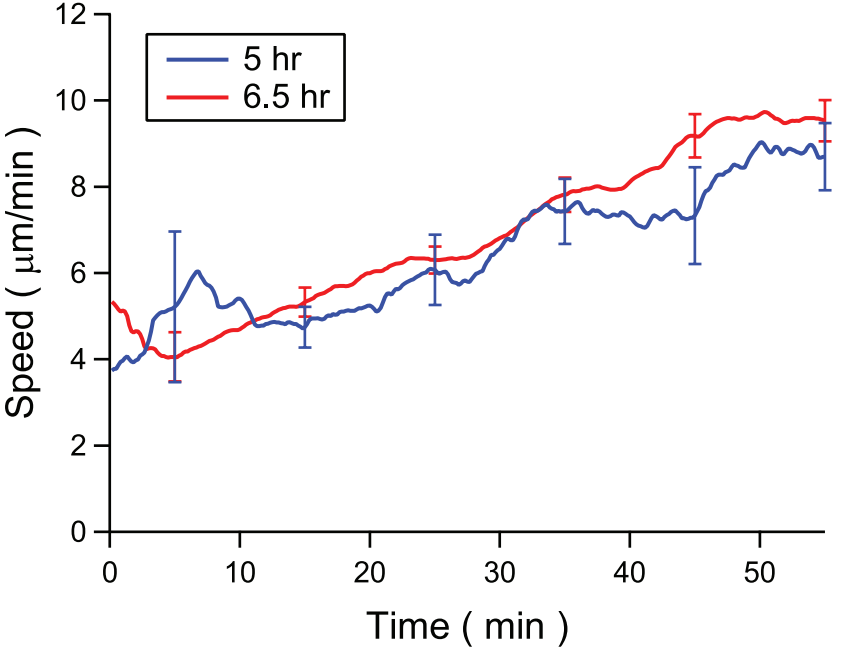
5 hr
6.5 hr
Speed (μm/min)
Time (min)
0
2
4
6
8
10
12
0
10
20
30
40
50